

not the same for each term; however, since the second-order term is the largest term in the multiple-scattering series, we will use the  $\langle r^{-1} \rangle$  calculated for second order. If we finally assume that only the  $S$ -wave part of  $t$  contributes, then the series can be summed in closed form.

The first term in the series is just  $T_{ss}$  and is given

$$P_1 = T_{ss} = \sum_j t(j) = A t_0 + (2i \cdot I) t_1, \quad (\text{A5})$$

where  $A$  is the number of nucleons,  $i$  is the isospin of the pion, and  $I$  is the isospin of the  $A$ -nucleon system. The double-scattering term is then

$$\begin{aligned} P_2 - \sum_{j \neq l} \sum_l t(j) t(l) \\ = A(A-1) t_0^2 + 2(A-1) t_0 t_1 (2i \cdot I) + [(2i \cdot I)^2 - A i^2] t_1^2. \end{aligned} \quad (\text{A6})$$

Note that the two-nucleon term  $P_2$  for the case  $I=0$  is

$$P_2^0 = A[(A-1) t_0^2 - i^2 t_1^2]. \quad (\text{A7})$$

The  $t_1$  part dominates  $P_2$  for small nuclei; thus, we observe that  $P_2$  is almost proportional to the number of nuclei for small nucleus.

For higher  $P_n$ , a recursive relationship can be found between  $P_n$ ,  $P_{n-1}$ , and  $P_{n-2}$ . This relationship is

$$P_n = [(A-2) t_0 + (2i \cdot I) t_1] P_{n-1} + (A-1) (t_0^2 - i^2 t_1^2) P_{n-2}. \quad (\text{A8})$$

Using Eqs. (A3) and (A5)–(A7), the series for  $T$  can be summed in closed form. For the case  $I=0$ , the result of this summation is

$$T = A \frac{t_0 + \langle r^{-1} \rangle (t_0^2 - i^2 t_1^2)}{1 - (A-2) t_0 \langle r^{-1} \rangle - (A-1) (t_0^2 - i^2 t_1^2) \langle r^{-1} \rangle^2}. \quad (\text{A9})$$

As an example, substitute  $t_0$ ,  $t_1$ ,  $A$ , and  $\langle r^{-1} \rangle$  for  $\text{He}^4$  into Eq. (A9). We find that the rest of the series  $\sum_{n>2} P_n \langle r^{-1} \rangle^{n-1}$  is approximately 10% of  $P_1 + \langle r^{-1} \rangle P_2$  for this case and is of the opposite sign of these first two terms. Results for other light nuclei are shown in Table II.

## Gamma-Ray Transitions Involving Isobaric-Spin Mixed States in $\text{Be}^8$

W. E. SWEENEY, JR.,\* AND J. B. MARION

*Department of Physics and Astronomy, † University of Maryland, College Park, Maryland 20742*

(Received 19 June 1968; revised manuscript received 27 November 1968)

The cross sections for the reactions  $\text{Li}^7(p, \gamma)\text{Be}^{8*}$  (16.63 and 16.90 MeV)  $\rightarrow 2\alpha$  have been measured over the range of bombarding energies 0.441–2.45 MeV. The nonresonant portion of the cross section for the population of the 16.63-MeV level has been compared successfully with cross sections calculated on the assumption of an extranuclear direct-capture process. Resonant cross sections populating the 16.63- and 16.90-MeV levels of  $\text{Be}^8$  were measured at incident energies of 0.441, 1.03, and 1.89 MeV, corresponding to levels at 17.64, 18.15, and 18.9 MeV in  $\text{Be}^8$ . Partial widths and reduced matrix elements were calculated for the resonant contributions to the cross sections. The experimental results are consistent with the hypothesis of nearly maximal isobaric-spin mixing in the  $J^\pi=2^+$  levels of  $\text{Be}^8$  (16.63 and 16.90 MeV). There is no evidence for transitions from the  $J^\pi=3^+$  levels near 19 MeV to either of the 16-MeV states, but decay to these states was observed from a level (probably  $J^\pi=2^-$ ) at 18.9 MeV.

### I. INTRODUCTION

THE occurrence of isobaric-spin mixing in the  $J^\pi=2^+$   $\text{Be}^8$  levels at 16.63 and 16.90 MeV has been firmly established by a review<sup>1</sup> of the experimental evidence. A vital experimental result which led to the proposal of isobaric-spin mixing in these levels<sup>2</sup> was the strong

$\gamma$ -ray transition<sup>3–5</sup> between the  $J^\pi=1^+$   $\text{Be}^8$  level at 17.64 MeV (which is predominantly  $T=1$ ) and 16.63-MeV level (which must contain appreciable  $T=1$  strength analog to the  $\text{Li}^8$  and  $\text{B}^8$  ground states). This strong transition, later shown to be primarily an  $M1$  transition,<sup>6,7</sup> cannot connect two states of the same

\* Present address: Institute for Exploratory Research, U.S. Army Electronics Command, Fort Monmouth, N.J.

† Research supported in part by the U.S. Atomic Energy Commission under Contract No. AT-(40-1)-2098.

<sup>1</sup> J. B. Marion and M. Wilson, Nucl. Phys. **77**, 129 (1966).

<sup>2</sup> J. B. Marion, Phys. Letters **14**, 315 (1965).

<sup>3</sup> P. Paul, S. L. Blatt, and D. Kohler, Phys. Letters **10**, 201 (1964).

<sup>4</sup> M. Wilson and J. B. Marion, Phys. Letters **14**, 313 (1965).

<sup>5</sup> D. Kohler and P. Paul, Phys. Letters **15**, 157 (1965).

<sup>6</sup> W. E. Sweeney, Jr., and J. B. Marion, Phys. Letters **19**, 243 (1965).

<sup>7</sup> W. E. Sweeney, Jr., following paper, Phys. Rev. **182**, 1022, (1969).

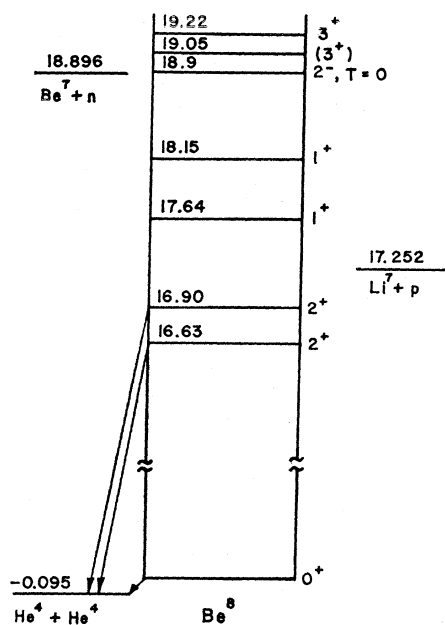


FIG. 1. Abbreviated energy-level diagram for  $\text{Be}^8$ .

isobaric spin without violating Morpurgo's rule<sup>8</sup> which states that  $\Delta T=0$ ,  $M1$  transitions are strongly inhibited in self-conjugate nuclei. The proposed model<sup>2</sup> that the 16-MeV levels of  $\text{Be}^8$  have essentially single-particle descriptions, with the 16.63-MeV level being mainly composed of the configuration  $\text{Li}^7+p$  and the 16.90-MeV level being mainly composed of the configuration  $\text{Be}^7+n$ , was further substantiated by the preliminary results of Marion and Wilson,<sup>1</sup> which indicated that the 16.63-MeV level, but not the 16.90-MeV level, was populated for all incident proton energies 0.65–2.4 MeV through the  $\text{Li}^7(p, \gamma)\text{Be}^{8*}$  capture reaction. This result can be attributed to a direct radiative capture reaction of the type which has been observed to occur in many light nuclei. Further evidence for a direct-capture transition to the 16.63-MeV level was provided by Paul *et al.*<sup>9</sup> They also observed<sup>10</sup> resonant transitions to the 16.63- and 16.90-MeV levels proceeding through the  $J^\pi=1^+$ , 18.15-MeV state.

In addition to the  $2^+$  doublet in  $\text{Be}^8$  there is also a  $1^+$  doublet at 17.64–18.15 MeV and possibly a  $3^+$  doublet at 19.05–19.22 MeV.<sup>11</sup> The possibility of isobaric-spin mixing has also been proposed<sup>2,10,12</sup> for these levels. A detailed knowledge of the  $\gamma$ -ray transitions between these three sets of doublets can provide useful information concerning the isobaric-spin mixing of the levels

since no *a priori* knowledge of the reaction amplitudes populating the states is needed for the analysis.

In the work presented here the differential cross sections for the  $\text{Li}^7(p, \gamma)\text{Be}^{8*}$  reactions leading to the 16.63- and 16.90-MeV states were measured as functions of the incident proton energy from the 0.441-MeV resonance to 2.45 MeV. The cross sections were measured by using a magnetic spectrometer and position-sensitive detector to observe the  $\alpha$  particles from the breakup of the 16-MeV levels. Resonant  $(p, \gamma)$  reactions leading to both the 16.63- and 16.90-MeV states were observed at proton energies of 0.441, 1.03, and 1.89 MeV corresponding to the formation of the  $J^\pi=1^+$ , 17.64-MeV,  $J^\pi=1^+$ , 18.15-MeV, and ( $J^\pi=2^-$ ), 18.9-MeV levels in  $\text{Be}^8$ . Partial widths and reduced matrix elements are presented for the resonant transitions. A nonresonant  $(p, \gamma)$  reaction leading to the 16.63-MeV level was observed at all proton energies and was successfully compared with the cross sections predicted by an extranuclear direct capture mechanism. Figure 1 is an abbreviated energy-level diagram of  $\text{Be}^8$  showing the levels of interest.

Angular correlations between the  $\gamma$  radiation and the breakup  $\alpha$  particles from the 16.63-MeV level were measured at the 0.441-MeV resonance and at an incident proton energy of 1.50 MeV. These results are contained in the following paper.<sup>7</sup> The differential cross-section calculations presented here depend on the angular-correlation results.

## II. EXPERIMENTAL PROCEDURES

### A. General

All experimental data were taken using the University of Maryland 3-MV Van de Graaff accelerator. The ion beam was analyzed by a  $90^\circ$  deflecting magnet and the regulated beam had an energy spread of less than 1 keV. Directly in front of the target chamber, a collimating system was used to produce a circular beam spot, the diameter of which could be varied from  $\frac{1}{8}$  to  $\frac{1}{4}$  in.

### B. Targets

Because of the low cross sections for the reactions  $\text{Li}^7(p, \gamma)\text{Be}^{8*}$  (16.63 and 16.90 MeV)  $\rightarrow 2\alpha$ , it was necessary to require the following of the target-detector system: (1) sufficient yield per unit incident beam, (2) total target and solid-angle contribution to the linewidth small enough to permit resolution of the  $\alpha$  particles from the 16.63- and 16.90-MeV states in  $\text{Be}^8$ , and (3) minimum target deterioration due to beam bombardment heating. Several combinations of target materials and target backings were investigated. The quality of the various targets was determined by analyzing the momentum distribution of  $\alpha$  particles from reaction  $\text{Li}^7(p, \alpha)\text{He}^4$ . The  $\alpha$ -particle spectrum from

<sup>8</sup> G. Morpurgo, Phys. Rev. **110**, 721 (1958).

<sup>9</sup> P. Paul, D. Kohler, and K. A. Snover, Bull. Am. Phys. Soc. **11**, 26 (1966).

<sup>10</sup> P. Paul, Naturforsch. **21a**, 914 (1966).

<sup>11</sup> T. Lauritsen and F. Ajzenberg-Selove, Nucl. Phys. **78**, 1 (1966).

<sup>12</sup> F. C. Barker, Nucl. Phys. **83**, 418 (1966).

this direct breakup reaction exhibits a significant low-energy tail<sup>1</sup> which for some targets was larger than the yield from the  $\text{Li}^7(p, \gamma)\text{Be}^{8*}$  (16.63 MeV) reaction. As a target deteriorates under beam bombardment, this low-energy tail increases in magnitude. Therefore, a fourth criterion for an acceptable target was that the breakup  $\alpha$  particles from the 16.63-MeV level be clearly visible above the tail of the direct breakup group.

These criteria were best fulfilled by lithium silicate targets evaporated on 0.010-in. thick tantalum backings. The targets were typically 20–25 keV thick to 0.441-MeV protons.

A lithium fluoride target was used to measure the absolute cross section of the  $\text{Li}^7(p, \alpha)\text{He}^4$  reaction at 0.880 MeV. Lithium fluoride is not as stable under beam bombardment as lithium silicate; however, the target thickness could be measured with greater accuracy by measuring the  $\gamma$ -ray yield from the  $\text{F}^{19}(p, \alpha\gamma)\text{O}^{16}$  resonance at 872.1 keV, which has a laboratory width of  $\Gamma = 4.7 \pm 0.2$  keV.<sup>13</sup>

### C. Apparatus and Procedure

The reaction chamber that was used is connected via a sliding seal assembly to a vertical double-focusing 180° magnetic spectrometer<sup>14</sup> which has a mean central radius of 20 in. The value of the magnetic field was determined by using a potentiometer to measure the voltage across a Hall probe which is enclosed in a constant-temperature oven. A feedback circuit was used to stabilize the magnet current to 1 part in 10<sup>5</sup>. For most of the measurements the spectrometer was placed at an angle of 120° with respect to the incident beam, which is close to the maximum angle permitted by the mechanical mount of the spectrometer. Since the fractional momentum spread of the three  $\alpha$ -particle groups increases with increasing angle, it is easier to resolve the three groups at a backward angle. The entrance aperture to the magnet consists of two sets of continuously adjustable slits which define a rectangular aperture at a distance of 8.0 in. from the center of the scattering chamber.

The  $\alpha$  particles were detected at the exit of the magnet by a 5×50 mm position-sensitive detector<sup>15</sup> with a depletion depth of 120  $\mu$ . A 5 in. diam×5 in. NaI(Tl) crystal was mounted outside the scattering chamber to serve as a monitor of the target condition.

The position and energy pulses from the detector were amplified by charge-sensitive low-noise preamplifiers and transmitted to linear amplifiers. Prompt bipolar outputs from the amplifiers were fed to separate analog-to-digital converters of a multiparameter ana-

lyzer system.<sup>16</sup> The data were stored in a 64×64 channel array. The two converters were operated in an internal slow-coincidence mode such that both a position pulse and an energy pulse must be present before storage occurs. Since the detection of a charged particle produces two simultaneous pulses, no external coincidence circuitry was required.

An ideal position-sensitive detector would produce, for monoenergetic incident particles, an energy  $E$  pulse which is constant over the active area of the detector and a position  $P$  pulse which varies linearly with distance along the position-sensitive direction:

$$P = (X/L)E, \quad (1)$$

where  $L$  is the length of the detector and  $X$  is the distance along the position-sensitive dimension. Since other observers<sup>17</sup> have experienced anomalies in the behavior of position-sensitive detectors, it was necessary to examine carefully the characteristics of this detector.

In order to calibrate the position-sensitive detector, the detector was mounted at the exit of the magnetic spectrometer on a rod which could be moved from outside the chamber. A lithium silicate target was bombarded with 1.25-MeV protons and the field of the spectrometer set such that 8.3-MeV  $\alpha$  particles from the  $\text{Li}^7(p, \alpha)\text{He}^4$  reaction would be focused along the central ray of the spectrometer. A small exit slit, 0.030 in. in height and centered on the central ray, allowed a small portion of the  $\alpha$ -particle spectrum to strike the detector. In this manner the  $\alpha$  particles which were detected had an energy spread of only 6 keV and a spatial spread of approximately 0.030 in. It was observed that the energy pulses increased in value at both ends of the detector and that the position pulses did not fall on a straight line; however, the spatial position of each detected  $\alpha$  particle could be determined from the ratio of the position and energy pulses. Figure 2 is a typical calibration curve for the position-sensitive detector showing the ratio of the position pulse to the energy pulse as a function of the distance along the position-sensitive dimension.

In order to obtain maximum yield while maintaining sufficient resolution, data were taken to determine the effect of target angle and entrance slit settings on the spatial distribution of  $\alpha$  particles from the  $\text{Li}^7(p, \alpha)\text{He}^4$  reaction. It was determined that a 1.6-in. vertical×0.25-in. horizontal entrance aperture and a target angle of 40° would not seriously reduce the resolution of the system and these values were used for the high-resolution measurements at 0.441, 0.650, 1.030, and 1.400 MeV. A somewhat larger aperture was used for the low-resolution measurements at all other energies.

<sup>13</sup> J. B. Marion, *Revs. Mod. Phys.* **38**, 660 (1966).

<sup>14</sup> V. LaTorre Aguilar, Ph.D. thesis, University of Maryland, 1965 (unpublished).

<sup>15</sup> Nuclear Diodes, Prairie View, Ill.

<sup>16</sup> Packard Instrument Co., Downers Grove, Ill.

<sup>17</sup> T. B. Clegg, A. C. L. Barnard, and J. B. Swint, *Nucl. Instr. Methods* **40**, 45 (1966).

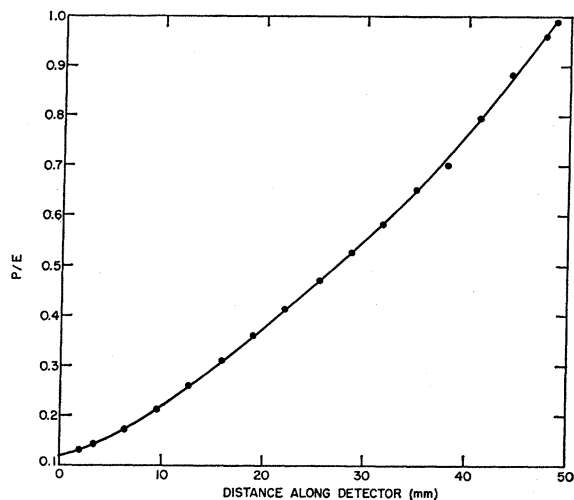


FIG. 2. Position pulse divided by energy-pulse calibration curve for a position-sensitive detector.

In the energy region 1.5–2.0 MeV,  $\alpha$  particles from the reaction  $F^{19}(p, \alpha)O^{16}$  have, at a laboratory angle of  $120^\circ$ , energies quite close to the energies of the  $\alpha$  particles from the 16.63- and 16.90-MeV levels of  $Be^8$ . The fluoride contamination in the targets, although small, was sufficient to eliminate the possibility of measuring the 16.63- and 16.90-MeV cross sections at this angle. Therefore, the cross-section measurements in this energy region were obtained at a detection angle of  $90^\circ$ . A measurement was also made at 1.400 MeV to allow for comparison with the  $120^\circ$  data.

The  $Li^7(p, \alpha)He^4$  direct breakup reaction was used to normalize the cross-section data. Data were accumulated for a total incident charge of  $10^9 \mu C$  both in the two-dimensional analyzer and in a scaler. A normalization measurement under identical conditions was made at the end of the  $Li^7(p, \gamma)Be^{8*}$  cross-section measurement. If the total charge required to obtain sufficient data was large, additional target normalizations were obtained at intermediate times using only the scaler. In general the total target deterioration was less than 10% for any measurement. Following the normalization measurement, the spectrometer was adjusted to detect the  $\alpha$  particles from the breakup of the 16.63- and 16.90-MeV levels of  $Be^8$ . Data were accumulated in units of 20 mC of beam charge until a sufficient number of counts was obtained.

#### D. Absolute Cross-Section Measurement

The absolute cross section for the reaction  $Li^7(p, \alpha)He^4$  was measured at an incident proton energy of 880 keV and a laboratory angle of  $120^\circ$ . The  $\alpha$  particles from a LiF target were momentum analyzed by the magnetic spectrometer and detected by a solid-state detector which was masked to yield an effective detector area of  $33 \times 10$  mm. The solid angle was defined by a 0.125-in.-

diam circular aperture placed  $2.698 \pm 0.032$  in. from the target. The combination of a large detector at the exit of the magnet and a small entrance aperture made possible the total collection of the  $\alpha$ -particle peak.

The absolute cross-section data were accumulated in the following manner. The thickness of a LiF target was determined by measuring the width of the  $\gamma$ -ray yield curve at the 0.872-MeV  $F^{19}(p, \alpha\gamma)O^{16}$  resonance. The proton energy was then set at 880 keV and the  $\alpha$ -particle yield from the  $Li^7(p, \alpha)He^4$  reaction was measured in units of  $50 \mu C$  of incident beam until a total charge of  $1500 \mu C$  was accumulated. A NaI crystal was used to monitor the  $\gamma$ -ray counting rate. The data were accumulated in  $50\text{-}\mu C$  units so that the  $\alpha$ -particle and  $\gamma$ -ray yields could be monitored to indicate any target deterioration; none was observed. The target thickness was remeasured and found to be the same as before within the accuracy of the measurement. The  $Li^7(p, \alpha)He^4$  yield was measured for an additional  $1500 \mu C$  of incident beam,  $500 \mu C$  at a time. The total yield of  $\alpha$  particles for the second measurement differed from the first by less than 1%.

The cross section for the  $Li^7(p, \alpha)He^4$  reaction was also measured as a function of incident proton energy from 0.441 to 2.45 MeV. The target was lithium silicate evaporated on a thick tantalum backing and had a thickness of approximately 20 keV to 0.441-MeV protons. The beam current was maintained below  $0.7 \mu A$  in order to prevent target deterioration. The cross section was measured at  $120^\circ$  from 0.441 to 2.45 MeV, and at  $90^\circ$  from 1.40 to 1.95 MeV. Some energies were repeated to check for target deterioration and for consistency of the measurements.

### III. EXPERIMENTAL RESULTS

#### A. Cross Section for the $Li^7(p, \alpha)He^4$ Reaction

Since the solid-state detector at the exit of the spectrometer collected all of the  $\alpha$  particles which passed through the small aperture in the scattering chamber, the laboratory differential cross section for the reaction is given by

$$\frac{d\sigma}{d\Omega} = \frac{\text{yield}/q(\mu C)}{\xi(\text{keV})} \times \frac{\epsilon(\text{keV cm}^2/\text{molecule})}{\text{No. of protons}/\mu C} \\ \times \frac{4r^2}{\pi d^2} \times \frac{1}{2} \times \frac{1}{0.925}, \quad (2)$$

where  $\xi$  is the energy loss in the LiF target of 880-keV protons,  $r$  ( $=2.698$  in.) is the distance from the target spot to the circular aperture whose diameter is  $d$  ( $=0.125$  in.), and  $\epsilon$  is the stopping cross section of LiF for 880-keV protons. The factor  $\frac{1}{2}$  is included since two  $\alpha$  particles are emitted per reaction. The factor  $1/0.925$  must be included since natural lithium, which contains 92.5%  $Li^7$ , was used for the LiF targets.

The width of the  $\gamma$ -ray yield curves for the  $\text{F}^{19}(p, \alpha\gamma)\text{O}^{16}$  reaction could be determined to an accuracy of 2.3% and the target thickness was determined to be  $(13.2 \pm 2.6\%)$  keV. The largest uncertainty in the determination of the absolute cross section comes from a lack of knowledge of the stopping cross section of LiF for 880-keV protons. Bader *et al.*<sup>18</sup> have measured the stopping cross section of LiF up to a proton energy of 600 keV. These data can be reproduced with reasonable accuracy by an expression of the type used by Whaling.<sup>19</sup> If this calculation is extended to 880-keV protons, it yields  $\epsilon = 9.61 \times 10^{-15}$  eV cm<sup>2</sup>/molecule. Tables of calculated stopping cross sections<sup>20</sup> yield a value of  $\epsilon = 9.58 \times 10^{-15}$  eV cm<sup>2</sup>/molecule. The absolute cross section of the  $\text{Li}^7(p, \alpha)\text{He}^4$  reaction at 880 keV calculated from an average of the above values is  $d\sigma/d\Omega = 0.473 \pm 5.4\%$  mb/sr, where the assigned error includes an estimated uncertainty of 4% in the stopping cross section. Using this normalization, the  $\text{Li}^7(p, \alpha)\text{He}^4$  cross sections at 90° and 120° are displayed in Fig. 3 and are tabulated in Table I.

### B. Reduction of the $P/E$ Data

Because of the nonlinearity of the  $P/E$ -versus-distance calibration of the position-sensitive detector, it was necessary to use the calibration curve to change the experimental data from "number of counts as a function of  $P/E$ " to "number of counts as a function of distance along the detector." This was accomplished by dividing the position-sensitive dimension of the detector into 40 equal intervals, 1.25 mm in length. From the  $P/E$ -versus-distance calibration curve,  $P/E$  values were assigned to the endpoints of the 40 intervals. The calibration curve was folded into the data

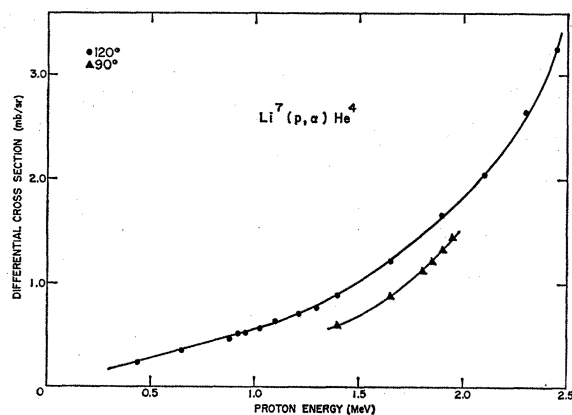


FIG. 3. Laboratory differential cross sections for the reaction  $\text{Li}^7(p, \alpha)\text{He}^4$ .

<sup>18</sup> M. Bader, R. E. Pixley, F. S. Mozer, and W. Whaling, *Phys. Rev.* **103**, 32 (1956).

<sup>19</sup> W. Whaling, *Encyclopedia of Physics*, edited by S. Flugge (Springer-Verlag, Berlin, 1958), Vol. XXXIV.

<sup>20</sup> C. Williamson and J. P. Boujot, Centre d'Etudes Atomiques, CEA Report No. 2189, 1962 (unpublished).

TABLE I. Laboratory differential cross sections for  $\text{Li}^7(p, \alpha)\text{He}^4$  reaction.

| Proton energy<br>(MeV) | 120° Data                    |  |
|------------------------|------------------------------|--|
|                        | $d\sigma/d\Omega$<br>(mb/sr) |  |
| 0.440                  | 0.236±0.013                  |  |
| 0.650                  | 0.353±0.019                  |  |
| 0.880                  | 0.473±0.026                  |  |
| 0.925                  | 0.510±0.028                  |  |
| 0.957                  | 0.532±0.029                  |  |
| 1.03                   | 0.571±0.031                  |  |
| 1.10                   | 0.623±0.034                  |  |
| 1.20                   | 0.704±0.038                  |  |
| 1.30                   | 0.772±0.042                  |  |
| 1.40                   | 0.885±0.048                  |  |
| 1.65                   | 1.213±0.066                  |  |
| 1.90                   | 1.654±0.090                  |  |
| 2.10                   | 2.04±0.11                    |  |
| 2.30                   | 2.68±0.14                    |  |
| 2.45                   | 3.26±0.18                    |  |
|                        | 90° Data                     |  |
| 1.40                   | 0.601±0.033                  |  |
| 1.65                   | 0.887±0.048                  |  |
| 1.80                   | 1.115±0.061                  |  |
| 1.85                   | 1.22±0.07                    |  |
| 1.90                   | 1.33±0.07                    |  |
| 1.95                   | 1.44±0.08                    |  |

by calculating the range of  $P/E$  values associated with each channel in the array and computing the overlap between the range of  $P/E$  values of the channel and the ranges of  $P/E$  values of the appropriate distance intervals. The counts were assigned to the correct intervals in proportion to the amount of overlap of the ranges.

### C. High-Resolution Measurements

In order to determine the branching ratio of  $\gamma$ -ray decay from the 18.15-MeV level to the 16.90- and 16.63-MeV levels of Be<sup>8</sup>, high-resolution cross section measurements were obtained at a laboratory angle of 120° for incident proton energies of 0.650, 1.030, and 1.400 MeV. The number of  $\alpha$  particles detected per 1.25-mm interval are shown in Figs. 4(a) and 4(b) for the data obtained at  $E_p = 0.650$  and 1.030 MeV, respectively. These data represent total charge accumulations of 0.3 C, requiring approximately 26 and 46 h of running time, at the two energies.

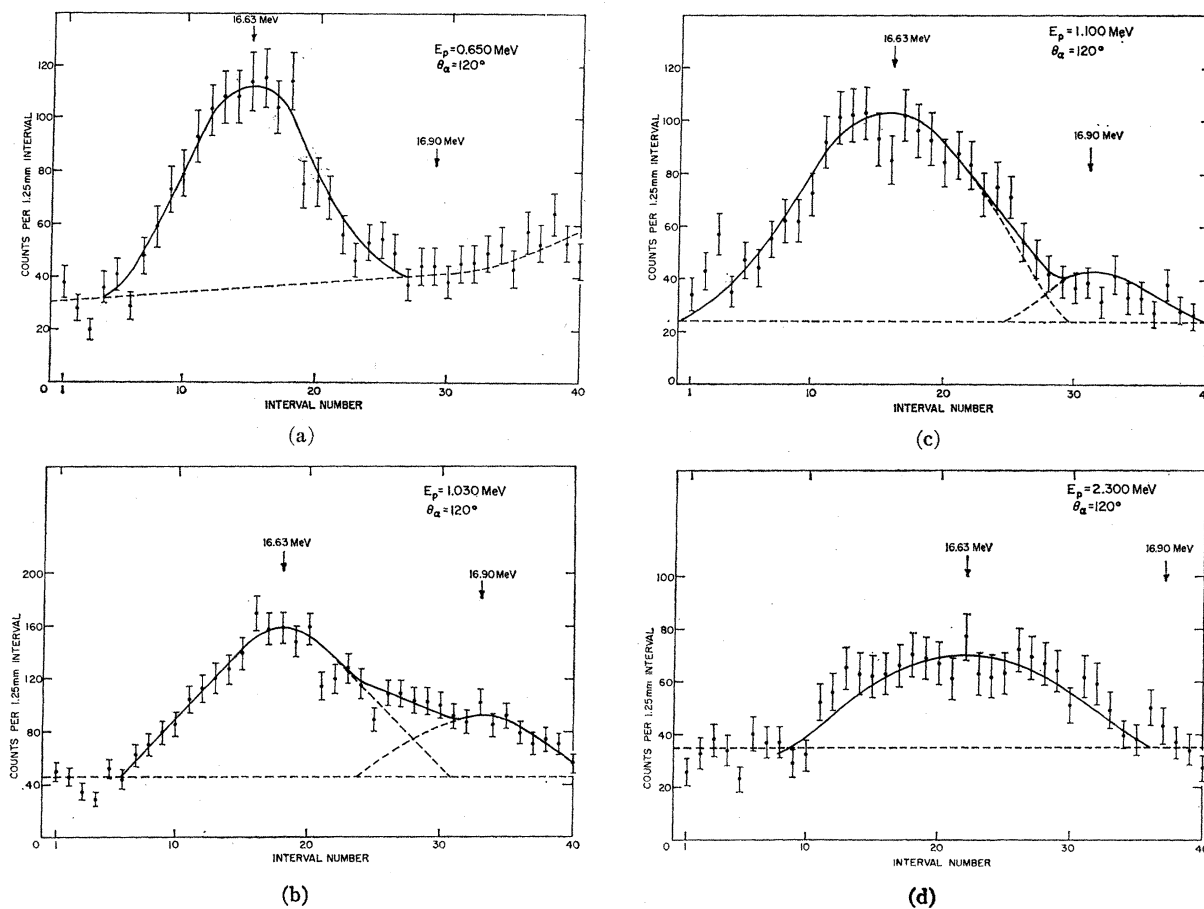


FIG. 4. Alpha-particle yields per 1.25-mm interval along the position-sensitive detector.

Since the breakup  $\alpha$  particles from the 16.63- and 16.90-MeV levels lie on a continuous background of direct breakup  $\alpha$  particles, it was necessary to determine the magnitude of this background for each data set. An attempt was made to choose a magnetic field strength such that the breakup  $\alpha$ -particle peaks from both of the 16-MeV levels would be entirely within the length of the detector. This attempt was usually successful below 2.10 MeV, and the high- and low-momenta backgrounds agreed within statistical uncertainty. When both high- and low-momenta backgrounds were visible, the average number of background counts per interval was taken to be the unweighted mean of the high- and low-momenta backgrounds.

If the background was not visible both above and below the  $\alpha$ -particle peaks, whichever background was visible was taken as the average. An exception to these two cases occurred at an incident proton energy of 0.650 MeV. As indicated by the dashed line in Fig. 4(a), the 16.63-MeV breakup  $\alpha$  particles lie on a sloping background. The calculation of the direct breakup background is a major source of uncertainty in the measurements.

The yield of breakup  $\alpha$  particles from the two 16-MeV levels were determined by summing over the appropriate intervals and subtracting the average background. For the cases in which the two peaks overlapped, as in Fig. 4(b), approximate line shapes were drawn and the counts in the intervals of overlap were distributed in proportion to the heights of the individual curves. It has been pointed out<sup>12,21</sup> that interference between the 16.63- and 16.90-MeV levels can be observed in the energy spectrum of reaction products from these levels. The calculation of this interference depends on definite knowledge of the level properties and reaction dynamics. Lacking the detailed knowledge necessary to calculate the interference correctly and considering the inherent resolution of the experimental arrangement, no attempt was made to correct for interference.

#### D. Low-Resolution Measurements

Low-resolution measurements of the cross sections for the  $\text{Li}^7(p, \gamma)\text{Be}^{8*}$  reactions leading to the 16.63-

<sup>21</sup> J. B. Marion, P. H. Nettles, C. L. Cocke, and G. J. Stephenson, Jr., *Phys. Rev.* **157**, 847 (1967).

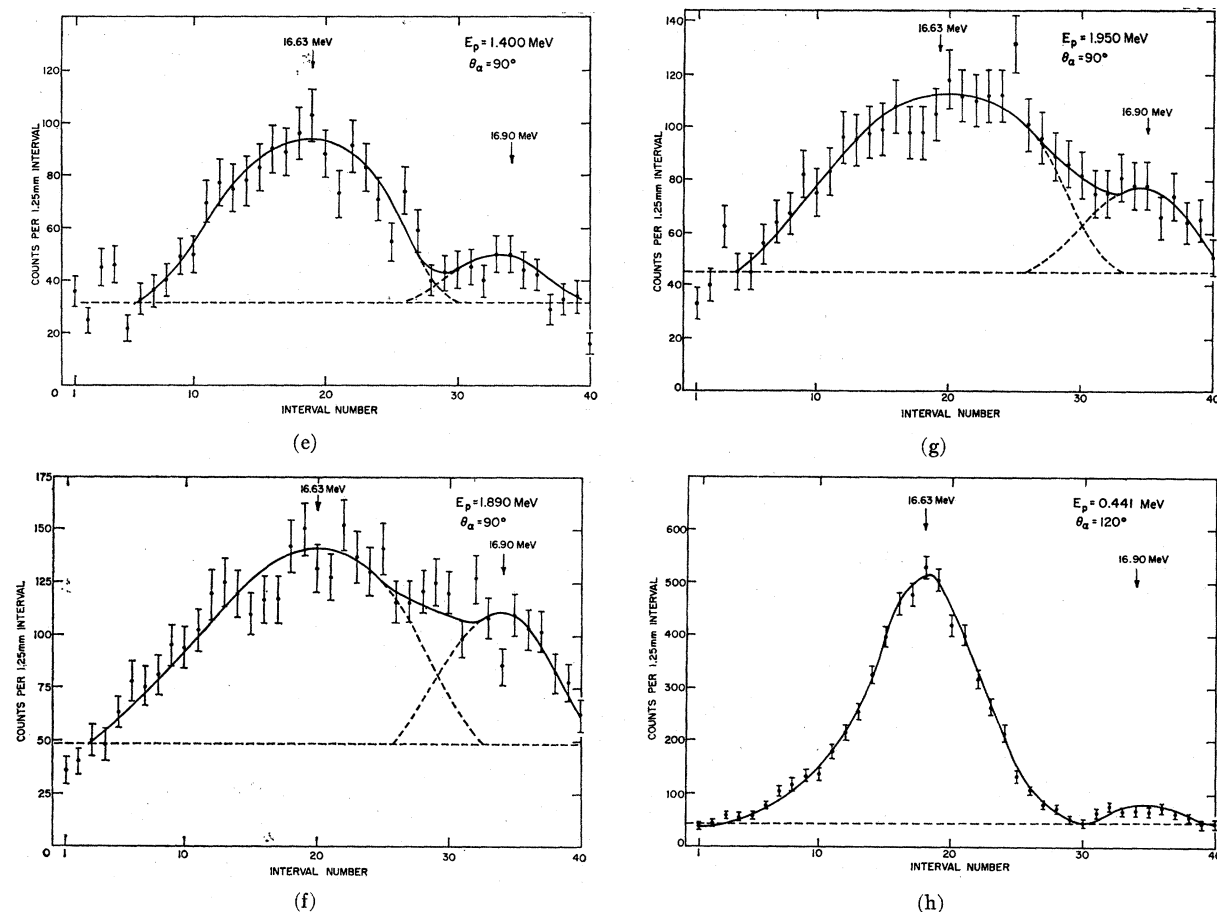


FIG. 4. (Continued).

and 16.90-MeV levels of  $\text{Be}^8$  were made at incident proton energies of 0.845, 0.957, 1.010, 1.100, and 1.210 MeV. The entrance aperture to the magnetic spectrometer for these measurements was  $1.6 \times 0.50$  in. and produced broader  $\alpha$ -particle peaks with consequent poorer resolution between the two peaks. Figure 4(c), which is typical of the low-resolution data, shows the data obtained at  $E_p = 1.10$  MeV. The poor resolution precludes a precise determination of the cross section to the 16.90-MeV level but has little effect on the determination of the cross section to the 16.63-MeV level. The background calculations and yield summations were carried out in a manner identical to that used with the high-resolution data.

Additional measurements at  $120^\circ$  of the cross sections for the  $\text{Li}^7(p, \gamma)\text{Be}^{8*}$  reaction proceeding through the 16.63-MeV level of  $\text{Be}^8$  were obtained at  $E_p = 2.100$ , 2.300, and 2.450 MeV. Because of the increased spatial spread of the breakup  $\alpha$ -particle peaks at higher energies, no attempt was made to detect all of the  $\alpha$  particles from the 16.90-MeV level; however, the magnetic spectrometer field setting was chosen so that any appreciable cross section for feeding the 16.90-MeV level would

have been observed. Figure 4(d) shows the data taken at an incident proton energy of 2.30 MeV. These data are typical of the data at higher energies.

#### E. Cross Sections at $90^\circ$

As previously mentioned, in the energy region 1.5–2.0 MeV it is necessary to select a detector angle other than  $120^\circ$  in order to separate the breakup  $\alpha$  particles from the 16-MeV states of  $\text{Be}^8$  from the  $\alpha$  particles from the  $\text{F}^{19}(p, \alpha_0)\text{O}^{16}$  reaction. Initially, cross-section measurements were obtained at 1.400, 1.650, and 1.890 MeV. Figure 4(e) shows the data taken at 1.400 MeV. The results for a bombarding energy of 1.890 MeV indicated a cross section significantly greater than expected from a direct-capture reaction, but the data were difficult to analyze due to poor resolution. Additional measurements were obtained at proton energies of 1.800, 1.850, 1.890, and 1.950 MeV with a thinner target and a smaller entrance aperture. The data obtained at 1.890 and 1.950 MeV are shown in Figs. 4(f) and 4(g), respectively. The resolution was inferior to the resolution obtained at lower energies and at  $120^\circ$  but was sufficient to allow the extraction of cross sec-

TABLE II. Yield ratios and absolute laboratory differential cross sections for the  $\text{Li}^7(p, \gamma)\text{Be}^{8*}$  (16.63 and 16.90 MeV) reactions.

| Proton energy | 120° Data                              |  |  |  |
|---------------|--|--|--|--|
|               | $\alpha(16.63)/\alpha_{\text{direct}}$ | $\alpha(16.90)/\alpha_{\text{direct}}$ | $(d\sigma/d\Omega)_{16.63}$<br>( $\mu\text{b}/\text{sr}$ ) | $(d\sigma/d\Omega)_{16.90}$<br>( $\mu\text{b}/\text{sr}$ ) |
| 0.441         | $1.85 \times 10^{-3} \pm 4\%$          | $0.59 \times 10^{-4} \pm 28\%$         | $0.690 \pm 0.048$  | $0.022 \pm 0.006$  |
| 0.441         | $1.71 \times 10^{-3} \pm 7\%$          |  | $0.709 \pm 0.077$  |  |
| 0.650         | $1.75 \times 10^{-4} \pm 8\%$          |  | $0.062 \pm 0.006$  |  |
| 0.845         | $1.72 \times 10^{-4} \pm 7\%$          | $0.135 \times 10^{-4} \pm 64\%$        | $0.079 \pm 0.007$  | $0.0062 \pm 0.0040$  |
| 0.957         | $1.99 \times 10^{-4} \pm 7\%$          | $0.171 \times 10^{-4} \pm 70\%$        | $0.106 \pm 0.009$  | $0.0091 \pm 0.0064$  |
| 1.010         | $2.24 \times 10^{-4} \pm 8\%$          | $0.561 \times 10^{-4} \pm 15\%$        | $0.125 \pm 0.012$  | $0.0314 \pm 0.0050$  |
| 1.030         | $2.19 \times 10^{-4} \pm 6\%$          | $0.726 \times 10^{-4} \pm 9\%$         | $0.126 \pm 0.010$  | $0.0417 \pm 0.0044$  |
| 1.10          | $1.90 \times 10^{-4} \pm 7\%$          | $0.179 \times 10^{-4} \pm 62\%$        | $0.118 \pm 0.011$  | $0.0111 \pm 0.0070$  |
| 1.21          | $1.33 \times 10^{-4} \pm 7\%$          | $0.086 \times 10^{-4} \pm 80\%$        | $0.094 \pm 0.008$  | $0.0061 \pm 0.0050$  |
| 1.40          | $0.94 \times 10^{-4} \pm 7\%$          | $0.077 \times 10^{-4} \pm 36\%$        | $0.083 \pm 0.007$  | $0.0068 \pm 0.0025$  |
| 2.10          | $0.56 \times 10^{-4} \pm 10\%$         |  | $0.111 \pm 0.013$  |  |
| 2.30          | $0.49 \times 10^{-4} \pm 9\%$          |  | $0.131 \pm 0.014$  |  |
| 2.45          | $0.43 \times 10^{-4} \pm 11\%$         |  | $0.140 \pm 0.017$  |  |
|               | 90° Data                               |  |  |  |
| 1.40          | $1.61 \times 10^{-4} \pm 7\%$          | $0.18 \times 10^{-4} \pm 31\%$         | $0.097 \pm 0.009$  | $0.0108 \pm 0.0034$  |
| 1.65          | $1.21 \times 10^{-4} \pm 7\%$          |  | $0.107 \pm 0.010$  |  |
| 1.80          | $1.25 \times 10^{-4} \pm 9\%$          | $0.098 \times 10^{-4} \pm 40\%$        | $0.141 \pm 0.015$  | $0.0111 \pm 0.0045$  |
| 1.85          | $1.47 \times 10^{-4} \pm 7\%$          | $0.230 \times 10^{-4} \pm 20\%$        | $0.179 \pm 0.016$  | $0.0281 \pm 0.0058$  |
| 1.89          | $1.95 \times 10^{-4} \pm 6\%$          | $0.640 \times 10^{-4} \pm 9\%$         | $0.254 \pm 0.021$  | $0.0832 \pm 0.0087$  |
| 1.89          | $1.65 \times 10^{-4} \pm 10\%$         |  | $0.215 \pm 0.025$  |  |
| 1.95          | $1.39 \times 10^{-4} \pm 8\%$          | $0.320 \times 10^{-4} \pm 15\%$        | $0.200 \pm 0.019$  | $0.0461 \pm 0.0074$  |

tions. A resonant feeding of the 16.63- and 16.90-MeV levels for proton energies near 1.890 MeV was observed and will be discussed below.

### F. Cross Sections at the 0.441-MeV Resonance

The differential cross sections for the  $\text{Li}^7(p, \gamma)\text{Be}^{8*}$  reactions at the 0.441-MeV resonance were measured independently several times. It has been shown<sup>1</sup> that the yield of  $\alpha$  particles from the breakup of the 16.63-MeV level has the same variation with incident proton energy as the high-energy  $\gamma$  radiation due to transitions from the 17.64-MeV level to the ground and first excited states of  $\text{Be}^8$ . The laboratory width of the resonance at  $E_p=0.441$  MeV is  $12.2 \pm 0.5$  keV<sup>11</sup> which is approximately one-half as large as the energy loss in the targets used for the measurements reported here. The yield from the direct breakup reaction used to normalize the data, neglecting the slow variation in the direct breakup cross section, is directly proportional to the thickness of the target. However, the yields from the  $\text{Li}^7(p, \gamma)\text{Be}^{8*}$  reactions must be corrected for the effect of using a target whose thickness is

greater than the width of the resonance. The correction is given by the relation

$$\left(\frac{d\sigma}{d\Omega}\right)_{\text{meas}} = \left(\frac{d\sigma}{d\Omega}\right)_{E_R} \times \frac{\Gamma}{\xi} \tan^{-1}\left(\frac{\xi}{\Gamma}\right). \quad (3)$$

The spectrum of breakup  $\alpha$  particles from the 16.63- and 16.90-MeV levels at  $E_p=0.450$  MeV is shown in Fig. 4(h). These data were obtained using a 17-keV thick lithium silicate target. The high-resolution mode was used and 0.3 C of total charge was accumulated. Unfortunately, applying the target-thickness correction to the data introduces a significant amount of uncertainty into the cross-section calculation due to the uncertainty in the level width.

Table II lists the results of the cross-section measurements. The cross sections  $(d\sigma/d\Omega)_{16.63}$  and  $(d\sigma/d\Omega)_{16.90}$  include the statistical uncertainties in the measurements of the yield ratios,  $\alpha(16.63)/\alpha(\text{direct})$  and  $\alpha(16.90)/\alpha(\text{direct})$ , and the uncertainty in the  $\text{Li}^7(p, \alpha)\text{He}^4$  cross section. Figure 5 shows the measured laboratory differential cross sections for the reaction  $\text{Li}^7(p, \gamma)\text{Be}^{8*} (16.90 \text{ MeV}) \rightarrow 2\alpha$ .



## IV. ANALYSIS

## A. Nonresonant Differential Cross-Section Data

The measured differential cross sections for the  $\text{Li}^7(p, \gamma)\text{Be}^{8*}$  (16.63 MeV) reaction (Table II) exhibit a smooth variation with proton energy on which are superimposed three resonances. The assumption that the nonresonant background involves no nuclear interaction in the initial state insures that there is no spin-flip. This type of direct process has also been treated<sup>22,23</sup> assuming some spin-independent nuclear interaction in the initial state.

A direct capture ( $p, \gamma$ ) reaction from the ground state of  $\text{Li}^7$  to either of the  $2^+$  levels of  $\text{Be}^8$  near 16 MeV can proceed either by a combination of  $S$ - and  $D$ -wave capture with the emission of an  $E1$   $\gamma$ -ray or by  $P$ -wave capture with emission of either  $M1$  or  $E2$   $\gamma$  radiation. The  $E1$  transition is highly favored over either  $M1$  or  $E2$  and only  $E1$  transitions will be considered here.

The expression for the total cross section for a ( $p, \gamma$ ) reaction proceeding via an  $E1$  transition as given by Christy and Duck<sup>24</sup> can be applied to the specific case of  $\text{Li}^7(p, \gamma)\text{Be}^{8*}$ . The final expression is<sup>25,26</sup>

$$\sigma_1 = \frac{25\pi}{108} \left( \frac{E_\gamma}{\hbar c} \right)^3 \frac{e^2}{\hbar c} \frac{c}{v} \sum_{l_1} |R_{1f_i}(l_1)|^2 \times \langle l_1, l_2 \rangle \sum_j \langle CJT | C_0 J_0 T_0 \rangle_j^2, \quad (4)$$

where the symbol  $\langle l_1, l_2 \rangle$  means the greater of  $l_1$  and  $l_2$ .

The radial integrals  $R_{1f_i}(l)$  are given by

$$R_{1f_i}(l) = \int r^2 \frac{g_f^*(r) g_i(r)}{k} dr, \quad (5)$$

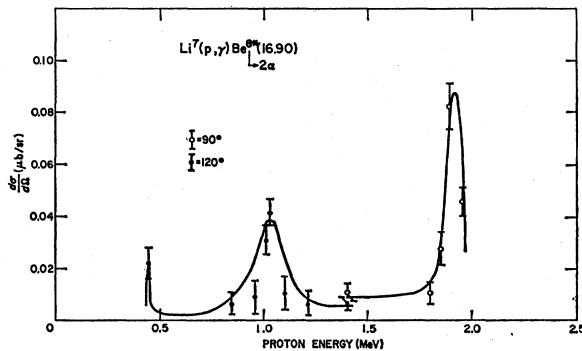


FIG. 5. Laboratory differential cross sections for the reaction  $\text{Li}^7(p, \gamma)\text{Be}^{8*}$  (16.90)  $\rightarrow 2\alpha$ .

<sup>22</sup> T. A. Tombrello, Nucl. Phys. **71**, 459 (1965).

<sup>23</sup> N. W. Tanner, Nucl. Phys. **63**, 383 (1965).

<sup>24</sup> R. F. Christy and I. Duck, Nucl. Phys. **24**, 89 (1961).

<sup>25</sup> This calculation is carried out in detail in Appendix D of Ref. 26.

<sup>26</sup> W. E. Sweeney, Jr., Ph.D. thesis, University of Maryland, 1967 (unpublished).

TABLE III. Coefficients of fractional parentage connecting the  $2^+$  states of  $\text{Be}^8$  to the ground state (g.s.) of  $\text{Li}^7$ .

| Be <sup>8</sup> state | cfp (Li <sup>7</sup> g.s.) |                 |
|-----------------------|----------------------------|-----------------|
|                       | $J=\frac{1}{2}$            | $J=\frac{3}{2}$ |
| $2^+, T=1$            | 0.13188                    | 0.48636         |
| $2^+, T=0$            | 0.20028                    | 0.43158         |

where

$$g_i(r) = F_h(kr) + [G_h(kr) + iF_h(kr)] \exp(i\delta_{J_i}) \sin\delta_{J_i}, \quad (6)$$

and  $g_f(r)$  is a bound-state wave function normalized to unity. The integrals can be evaluated using the code ABACUS-2,<sup>27</sup> where the matrix elements are related by

$$|R_{1f_i}|^2 = \frac{1}{4} \lambda^2 |\langle r \rangle|^2_{\text{ABACUS}}. \quad (7)$$

The bound state consists of an  $l=1$  proton bound in the well formed by the  $\text{Li}^7$  core. The interaction potential between the  $l=1$  proton and the  $\text{Li}^7$  core was taken to be a real Woods-Saxon nuclear potential plus the Coulomb potential of a uniformly charged sphere having the same radius as the Woods-Saxon well. The analysis by Tombrello<sup>22</sup> shows that the  $2^+$  levels in  $\text{Li}^8$  and  $\text{Be}^8$  can be reproduced with well depths of 32.89 and 32.62 meV, respectively. The well depth for the  $2^+$  level at 16.63 MeV in  $\text{Be}^8$  was taken to be 32.77 MeV. Following Tombrello, the nuclear radius was chosen to be 2.95 fm and the diffusivity was chosen to be 0.52 fm. The initial-state interaction was chosen to be just the Coulomb repulsion of a uniformly charged sphere also having a radius of 2.95 fm.

The strength of the direct-capture reaction is governed by the magnitude of the spectroscopic factor<sup>28</sup>  $S = \sum_j \langle CJT | C_0 J_0 T_0 \rangle_j^2$ , which measures how well the 16-MeV excited states of  $\text{Be}^8$  can be represented by the  $\text{Li}^7$  ground state plus an  $l=1$  proton. Stephenson and Marion<sup>29</sup> have used the shell-model wave functions of Barker<sup>12</sup> to calculate the coefficients of fractional parentage connecting the  $J^\pi=2^+, T=1$  and  $J^\pi=2^+, T=0$  states to the ground state of  $\text{Li}^7$ . Their results are shown in Table III.

The 16.63- and 16.90-MeV levels of  $\text{Be}^8$  can best be represented by<sup>21</sup>

$$|16.63\rangle = 0.772 |T=0\rangle + 0.636 |T=1\rangle,$$

$$|16.90\rangle = 0.636 |T=0\rangle - 0.772 |T=1\rangle. \quad (8)$$

The coefficients of fractional parentage for these levels

<sup>27</sup> E. H. Auerbach, ABACUS-2, Brookhaven National Laboratory Report No. BNL 6562, 1962 (unpublished).

<sup>28</sup> J. B. French, in *Nuclear Spectroscopy*, edited by F. Ajzenberg-Selove (Academic Press Inc., New York, 1960), Part B.

<sup>29</sup> G. J. Stephenson, Jr., and J. B. Marion (unpublished).

TABLE IV. Calculated cross sections for the direct-capture reaction  $\text{Li}^7(p, \gamma)\text{Be}^8$  (16.63 MeV) assuming a pure Coulomb potential and also a small nuclear potential.

| $E_p$<br>(MeV) | Coulomb potential                 |                                   |                                   | $\sigma_T$<br>( $\mu\text{b}$ ) | $d\sigma/d\Omega$<br>( $\mu\text{b}/\text{sr}$ ) | 3.45-MeV potential              |  |
|----------------|-----------------------------------|-----------------------------------|-----------------------------------|---------------------------------|--|---------------------------------|--|
|                | $\sigma_s/S$<br>( $\mu\text{b}$ ) | $\sigma_d/S$<br>( $\mu\text{b}$ ) | $\sigma_T/S$<br>( $\mu\text{b}$ ) |                                 |  | $\sigma_T$<br>( $\mu\text{b}$ ) | $d\sigma/d\Omega$<br>( $\mu\text{b}/\text{sr}$ ) |
| 0.2            | 0.204                             | 0.001                             | 0.205                             | 0.096                           | 0.0075   | 0.105                           | 0.0082   |
| 0.4            | 0.682                             | 0.064                             | 0.746                             | 0.351                           | 0.0251   | 0.397                           | 0.0307   |
| 0.6            | 1.046                             | 0.165                             | 1.211                             | 0.569                           | 0.0438   | 0.663                           | 0.0509   |
| 0.8            | 1.298                             | 0.297                             | 1.595                             | 0.750                           | 0.0574   | 0.884                           | 0.0676   |
| 1.0            | 1.462                             | 0.454                             | 1.916                             | 0.901                           | 0.0686   | 1.058                           | 0.0805   |
| 1.2            | 1.568                             | 0.621                             | 2.189                             | 1.029                           | 0.0779   | 1.191                           | 0.0901   |
|                |                                   |                                   |                                   |                                 | 0.090 <sup>a</sup>                               |                                 | 0.104 <sup>a</sup>                               |
| 1.4            | 1.642                             | 0.800                             | 2.442                             | 1.148                           | 0.0864   | 1.302                           | 0.0980   |
|                |                                   |                                   |                                   |                                 | 0.101 <sup>a</sup>                               |                                 | 0.115 <sup>a</sup>                               |
| 1.6            | 1.688                             | 0.974                             | 2.662                             | 1.251                           | 0.0936   | 1.386                           | 0.1037   |
|                |                                   |                                   |                                   |                                 | 0.113 <sup>a</sup>                               |                                 | 0.127 <sup>a</sup>                               |
| 1.8            | 1.710                             | 1.161                             | 2.871                             | 1.349                           | 0.1003   | 1.458                           | 0.1082   |
|                |                                   |                                   |                                   |                                 | 0.123 <sup>a</sup>                               |                                 | 0.136 <sup>a</sup>                               |
| 2.0            | 1.721                             | 1.340                             | 3.061                             | 1.439                           | 0.1060   | 1.515                           | 0.1117   |
|                |                                   |                                   |                                   |                                 | 0.128 <sup>a</sup>                               |                                 | 0.138 <sup>a</sup>                               |
| 2.2            | 1.728                             | 1.523                             | 3.251                             | 1.528                           | 0.1118   | 1.569                           | 0.1149   |
|                |                                   |                                   |                                   |                                 | 0.136 <sup>a</sup>                               |                                 | 0.143 <sup>a</sup>                               |
| 2.4            | 1.725                             | 1.708                             | 3.433                             | 1.614                           | 0.1171   | 1.618                           | 0.1171   |

<sup>a</sup> These values are for  $\theta_{\text{lab}} = 90^\circ$  all others for  $120^\circ$ .

are then found by relations of the form

$$\begin{aligned} \text{cfp}_j(16.63) &= 0.772\text{cfp}_j(T=0) + 0.636\text{cfp}_j(T=1), \\ \text{cfp}_j(16.90) &= 0.636\text{cfp}_j(T=0) - 0.772\text{cfp}_j(T=1). \end{aligned} \quad (9)$$

The spectroscopic factors as calculated by the relation  $S = \sum_j \text{cfp}^2(j)$  are

$$S(16.63) = 0.470, \quad S(16.90) = 0.010. \quad (10)$$

These values are in agreement with the model which represents the 16.63-MeV state of  $\text{Be}^8$  as  $\text{Li}^7 + p$  and the 16.90-MeV state of  $\text{Be}^8$  as  $\text{Be}^7 + n$ . On the basis of the spectroscopic factors alone (i.e., ignoring the difference in the radial matrix elements for the 16.63- and

16.90-MeV levels due to their different bound-state wave functions), one expects the direct capture cross section to the 16.90-MeV state of  $\text{Be}^8$  to be about 2% of the 16.63-MeV cross section. Table IV lists the calculated  $S$ -wave,  $D$ -wave, and total cross sections using the spectroscopic factor  $S = 0.470$ .

Before these calculated cross sections can be compared with the experimental results, they must be changed to differential cross sections at the appropriate angles. To determine the angular distribution of breakup  $\alpha$  particles following a direct-capture ( $p, \gamma$ ) reaction, it is only necessary to integrate Eq. (37) of the following paper over all possible directions of emission of the  $\gamma$  ray. Only those terms which contain a  $Y_0^0(\Omega_\gamma)$  are retained, yielding the angular distribution expression

$$\begin{aligned} 4\pi(d\sigma/d\Omega)_{\text{c.m.}}/\sigma T &= \left[ \frac{5}{2} |R(0)|^2 + 5 |R(2)|^2 - 2 |R(2)|^2 Q_2(\alpha) Y_2^0(\Omega_\alpha) \right. \\ &\quad \left. + (4/\sqrt{5}) Q_2(\alpha) Y_2^0(\Omega_\alpha) \cos(\delta_2 - \delta_0) R(0) R^*(2) \right] / \left[ \frac{5}{2} |R(0)|^2 + 5 |R(2)|^2 \right]. \end{aligned} \quad (11)$$

The angles  $\theta_\alpha$  and  $\phi_\alpha$  should be measured from the direction of recoil of the  $\text{Be}^8$  excited state, which depends on the direction of emission of the  $\gamma$  ray. A reasonable approximation is to neglect the recoil ve-

locity and assume that the  $\alpha$ -particle breakup occurs in the c.m. system. When the laboratory angle of detection of the  $\alpha$  particles is  $120^\circ$ , the spherical harmonics  $Y_2^0(\Omega_\alpha)$ , evaluated in the c.m. system, are of

the order  $-0.1$ ; consequently any uncertainty in the knowledge of the phase difference  $\delta_2 - \delta_0$  will have a negligible effect on the transformation to differential cross sections at  $120^\circ$ . At  $90^\circ$  in the laboratory, the values of  $Y_2^0(\Omega_\alpha)$  in the c.m. system are of the order  $-1.0$ ; therefore, the term containing  $\cos(\delta_2 - \delta_0)$  is significant.

The value of  $\delta_2 - \delta_0$  as a function of energy from 1.2 to 2.2 MeV was calculated in a manner identical to that used in Ref. 7 (i.e., the hard-sphere phase shifts were evaluated at 3 nuclear radii). The resonance near 1.89 MeV is attributed to  $S$ -wave protons and introduces an additional  $180^\circ$  shift in the  $S$ -wave phase above the resonance.

The final correction to be applied to the total cross-section data is the solid-angle transformation from the c.m. to the laboratory coordinate system. These transformation factors were also calculated by ignoring the recoil velocity of the Be<sup>8</sup> excited state. The calculated laboratory differential cross sections are also listed in Table IV.

The introduction of some nuclear potential in the initial state must now be considered. Higher-energy ( $\sim 10$  MeV) proton elastic-scattering data has been successfully reproduced<sup>30</sup> with an optical-model potential consisting of a large real well ( $\sim 60$  MeV), a surface absorption potential, and a strong spin-orbit potential ( $\sim 18$  MeV). The potentials necessary to account for the elastic-scattering data are energy-dependent and would be expected to be somewhat smaller at lower energies. However, the difficulties in fitting  $(p, \gamma)$  cross sections using elastic-scattering potentials has been demonstrated by Tanner,<sup>23</sup> and an attempt to fit the observed data with elastic-scattering potentials failed.

Tombrello<sup>22</sup> has been successful in reproducing the shape of the  $\text{Li}^7(n, \gamma)\text{Li}^8$  cross sections at low energies using a real Woods-Saxon well with  $V_0 = 3.56$  MeV for channel spin 2 and  $V_0 = 0$  for channel spin 1. The  $\text{Li}^7(p, \gamma)\text{Be}^{8*}(16.63 \text{ MeV})$  total and differential cross sections were recalculated using a real Woods-Saxon potential plus the Coulomb repulsion for the initial scattering state. The shape parameters were the same as for the bound-state potential, and the well depths were  $V_0 = 3.45$  MeV for channel spin 2 and  $V_0 = 0$  for channel spin 1. The results are listed in Table IV. Figure 6 shows the comparison between the experimental results and the cross sections calculated using only the Coulomb potential and using the small well plus the Coulomb potential. It should be noted that the agreement for the Coulomb potential could be significantly improved by increasing slightly the value of the spectroscopic factor. It is possible that a better fit could be obtained by varying the initial-state well depth; however, Tombrello has demonstrated that the

<sup>30</sup> R. Gleyvod, N. P. Heydenburg, and I. M. Naqib, Nucl. Phys. 63, 650 (1965).

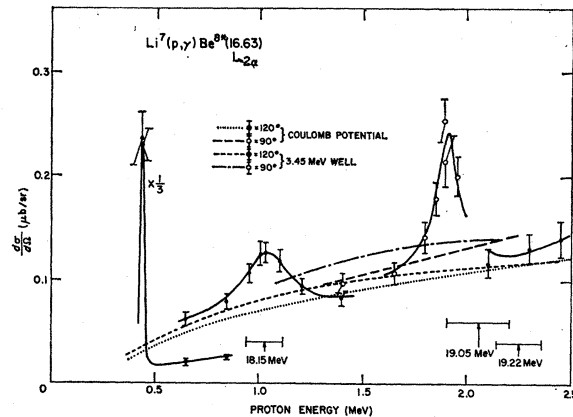


FIG. 6. Laboratory differential cross sections for the reaction  $\text{Li}^7(p, \gamma)\text{Be}^{8*}(16.63) \rightarrow 2\alpha$ . The dashed lines are calculated values assuming an extranuclear direct-capture process. The  $1^+$  level at 18.15 MeV and the  $3^+$  levels near 19 MeV are shown on the diagram.

calculated cross sections for  $\text{Be}^7(p, \gamma)\text{B}^8$  are virtually identical for initial-state well depths of 3.29 and 3.56 MeV, which indicates that a large change in well depth would be necessary to change significantly the values of the calculated cross section. In view of the fact that no parameters were varied in the cross-section calculations, other than the depth of the initial-state well, the reasonable agreement of the calculated cross sections with the experimental measurements of the nonresonant cross sections is a strong indication that the reaction proceeds by an extranuclear direct capture process.

### B. Resonant Differential Cross-Section Data

The attempt to reproduce the nonresonant cross sections for the  $\text{Li}^7(p, \gamma)\text{Be}^{8*}(16 \text{ MeV}) \rightarrow 2\alpha$  reactions is motivated by the desire to determine as precisely as possible the resonant contributions to these reactions. The first resonance occurs at an incident proton energy of 0.441 MeV and corresponds to the first  $J^\pi = 1^+$  level in Be<sup>8</sup> at 17.64 MeV. The difference in phase between  $S$  and  $P$  waves is known to pass through  $90^\circ$  near the 0.441-MeV resonance.<sup>31</sup> Thus, for a target which is somewhat thicker than the width of the resonance, any interference between the  $S$ -wave direct capture and the  $P$ -wave resonant cross sections will be quite small since the interference will be proportional to  $\cos(\delta_s - \delta_p)$ . The weighted average of the measurements reported here for the 16.63-MeV cross section at  $120^\circ$  is  $(d\sigma/d\Omega)_{\text{lab}} = 0.695 \pm 0.063 \mu\text{b}/\text{sr}$ . The subtraction from this cross section of the nonresonant background, as estimated from the average of the calculated cross section values obtained using a small attractive potential in the initial state and no nuclear potential in the initial state, yields for the resonant contribution to the

<sup>31</sup> B. Mainsbridge, Nucl. Phys. 21, 1 (1960).

laboratory cross section for the reaction  $\text{Li}^7(p, \gamma)\text{Be}^8$  (16.63 MeV)  $\rightarrow 2\alpha$  at the 0.441-MeV resonance  $(d\sigma/d\Omega)_{\text{lab}} = 0.663 \pm 0.063 \mu\text{b}/\text{sr}$ . Changing this to c.m. coordinates, the resonant cross section is  $(d\sigma/d\Omega)_{\text{c.m.}} = 0.684 \pm 0.065 \mu\text{b}/\text{sr}$ .

Finally, any anisotropy in the distribution of the resonant breakup  $\alpha$  particles must be accounted for. The expression for the angular distribution of the resonant breakup  $\alpha$  particles is

$$W(\theta_\alpha) = (1 + \delta^2)(1 + r) - (1 - \delta^2)P_2(\cos\theta_\alpha)(0.1r - 0.5), \quad (12)$$

where  $\delta$  is the  $E2/M1$  mixing ratio amplitude, and  $r$  is the channel-spin mixing ratio. The value of  $\delta^2$  is very nearly zero<sup>6,7</sup>; therefore, evaluating  $P_2(\cos\theta_\alpha)$  at the angle of emission of the  $\alpha$  particles with respect to the recoiling  $\text{Be}^8$  nucleus and using the value<sup>32</sup>  $r = 3.2$ , one obtains

$$\sigma(17.64-16.63) = 8.62 \pm 0.83 \mu\text{b}. \quad (13)$$

The total c.m. cross section for the 17.64–16.90  $\gamma$ -ray transition is calculated in a similar fashion. The laboratory differential cross section is  $(d\sigma/d\Omega)_{\text{lab}} = 0.022 \pm 0.006 \mu\text{b}/\text{sr}$ . Background from the direct-capture reaction to this state is negligibly small as verified by the cross-section measurement at an incident proton energy of 0.650 MeV. The angular distribution correction, which is very small, was calculated assuming a pure  $M1$  transition. With this assumption and applying the laboratory-to-c.m. correction, the resonant cross section for the 17.64–16.90 transition is found to be

$$\sigma(17.64-16.90) = 0.286 \pm 0.084 \mu\text{b}. \quad (14)$$

The resulting value of the branching ratio is

$$\sigma(17.64-16.90)/\sigma(17.64-16.63) = (3.3 \pm 1)\%. \quad (15)$$

The cross section to the 16.63-MeV state of  $\text{Be}^8$  was first measured to be  $11 \mu\text{b}$  by Paul *et al.*<sup>3,5</sup> Subsequently, Marion and Wilson<sup>1</sup> obtained a value of  $6.45 \pm 0.7 \mu\text{b}$ . However, the latter calculation did not include the correction for finite target thickness which can have a large effect on the measured value of the differential cross section at the peak of the 0.441-MeV resonance.

The branching ratio has also been measured by these authors. Kohler and Paul<sup>5</sup> obtained a value of  $(7.5 \pm 2)\%$ . Wilson and Marion obtained a value of  $(5.9 \pm 2)\%$  using a magnetic spectrometer and nuclear emulsions,<sup>4</sup> and a value of  $(7.6 \pm 1)\%$  using the magnetic spectrometer and a solid-state detector.<sup>1</sup> A re-examination of the data used to obtain the latter branching ratio reveals that an unduly optimistic value was placed on the uncertainty. Analysis of that data yields a branching ratio of  $(7.6 \pm 4)\%$ . The branching ratios reported in Refs. 1 and 4 and the present value

of  $(3.3 \pm 1)\%$  were all obtained using a magnetic spectrometer to analyze the  $\alpha$ -particle spectrum. The weighted mean of these measurements is  $(4.0 \pm 0.9)\%$ .

The branching ratio was also calculated from other data, not reported here, taken with the magnetic spectrometer and the position-sensitive detector. The uncertainties in these data were larger than in the data shown in Fig. 4(h); however, the values obtained for the branching ratio were always between 3 and 4%.

The measurement by Kohler and Paul was obtained by recording the spectrum of  $\gamma$  rays coincident with the breakup  $\alpha$  particles from the 16.63- and 16.90-MeV levels of  $\text{Be}^8$ . They obtained a yield for the 17.64–16.90 transition by stripping the 17.64–16.63  $\gamma$ -ray spectrum from their total spectrum. Since the energy of the 17.64–16.90  $\gamma$  ray nearly coincides with the energy of the Compton peak of the 17.64–16.63  $\gamma$  ray, this technique is sensitive to the level width of the 16.63-MeV state. The width of this level has recently been shown<sup>21,33</sup> to be about 110 keV, which is significantly larger than the best value for the level width (85 keV) at the time of their calculation. The use of a larger width would reduce their value for the branching ratio; however, they indicate<sup>34</sup> that the statistical accuracy of the available  $\gamma$ -ray spectra is insufficient to distinguish between the two values of the level width (i.e., 85 and 110 keV). Additional data obtained by the method of Paul *et al.* would be useful in clearing up the discrepancy in branching-ratio values obtained by recording the  $\alpha$ -particle spectrum as opposed to the  $\gamma$ -ray spectrum.

The next resonance occurs at an incident proton energy near 1.03 MeV and corresponds to the  $J^\pi = 1^+$  level at 18.15-MeV excitation energy in  $\text{Be}^8$ . At this energy the background direct-capture reaction has a significant contribution from both  $S$  and  $D$  waves, and the possibility of direct-compound interference in the differential cross section exists. However, since the  $\gamma$  rays are unobserved, the interference is restricted to the first stage of the reaction and is not expected to be strong. A further indication of the lack of a strong interference term is the lack of asymmetry in the shape of the excitation curve in the vicinity of the resonance.

The differential cross section for the 18.15–16.63-MeV transition was measured to be  $(d\sigma/d\Omega)_{\text{lab}} = 0.126 \pm 0.010 \mu\text{b}/\text{sr}$  at an incident proton energy of 1.03 MeV. The estimation of the direct-capture contribution to this cross section is difficult at best. The calculated direct-capture cross sections at 1.03 MeV are  $0.071 \mu\text{b}/\text{sr}$  for the case of Coulomb potential only and  $0.082 \mu\text{b}/\text{sr}$  for the case of Coulomb potential plus a small nuclear potential. The direct-capture contribution can also be

<sup>33</sup> C. P. Browne, W. D. Callender, and J. R. Erskine, Phys. Letters **23**, 371 (1966).

<sup>32</sup> V. Meyer, H. Müller, H. H. Staub, and R. Zurmühle, Nucl. Phys. **27**, 284 (1961).

<sup>34</sup> P. Paul, D. Kohler, and K. A. Snover, Phys. Rev. **173**, 919 (1968).

estimated directly from the data. The direct-capture contribution at 1.03 MeV found by connecting the experimental points at 0.650 and 1.40 MeV is 0.072  $\mu\text{b}/\text{sr}$ , while the contribution estimated from a smooth curve through the data points at 0.650, 0.845, and 1.210 MeV is 0.084  $\mu\text{b}/\text{sr}$ . From these four values one can obtain a reasonable estimate of  $0.077 \pm 0.007 \mu\text{b}/\text{sr}$ . Therefore, the resonant contribution is found to be  $(d\sigma/d\Omega)_{\text{lab}} = 0.049 \pm 0.012 \mu\text{b}/\text{sr}$ . At this energy and at a laboratory angle of  $120^\circ$  the value of  $P_2(\cos\theta)$  is nearly zero and no correction need be made other than the laboratory to c.m. solid-angle transformation. The total resonant cross section for the 18.15–16.63  $\gamma$ -ray transition is, therefore,

$$\sigma(18.15-16.63) = 0.65 \pm 0.16 \mu\text{b}. \quad (16)$$

For the 18.15–16.90  $\gamma$ -ray transition the measured differential cross section is  $0.0417 \pm 0.0044 \mu\text{b}/\text{sr}$ . The background direct-capture contribution is quite small. From the measured values at 0.650 and 1.40 MeV and from the ratio of the spectroscopic factors for the 16.90- and 16.63-MeV states of Be<sup>8</sup> and the estimate of the direct-capture contributions to the 16.63 level, the background contribution is estimated to be  $0.0025 \pm 0.0010 \mu\text{b}/\text{sr}$ . Therefore, the resonant differential cross section at  $120^\circ$  is  $(d\sigma/d\Omega)_{\text{lab}} = 0.0392 \pm 0.0046 \mu\text{b}/\text{sr}$ . Consequently, the total cross section for the 18.15–16.90  $\gamma$ -ray transition is

$$\sigma(18.15-16.90) = 0.52 \pm 0.06 \mu\text{b}. \quad (17)$$

The branching ratio is

$$\sigma(18.15-16.90)/\sigma(18.15-16.63) = 0.80 \pm 0.22. \quad (18)$$

A comparison can now be made between the results obtained here and those obtained by Paul *et al.*<sup>10,34</sup> They measured total cross sections of 11 and 2.2  $\mu\text{b}$  for the 17.64–16.63 and 18.15–16.63 transitions, respectively. These results are consistently 30% greater than the total cross sections obtained here. For the 18.15–16.63 transition, Paul *et al.* found that the direct-capture background was less than 50% of the total cross section, while the measurements reported here indicate that the direct-capture background is greater than 60% of the total cross section. They obtained resonant cross sections of  $\sigma(18.15-16.90) = 0.65 \pm 0.2 \mu\text{b}$  and  $\sigma(18.15-16.63) = 1.30 \pm 0.32 \mu\text{b}$  which yields a branching ratio of 0.5 compared with the value presented here of  $0.80 \pm 0.22$ . An increase in the amount of direct-capture background beneath the 18.15–16.63 resonant cross section in the data of Paul *et al.* would not only raise their branching ratio but also explain their observation of a laboratory resonant width for this reaction of  $230 \pm 50 \text{ keV}$  which is unaccountably large.

Paul *et al.*<sup>10,34</sup> obtained their absolute cross sections by normalizing to the yield from the  $\text{F}^{19}(p, \alpha_0)\text{O}^{16}$  reaction. The cross section for this reaction at  $E_p = 1.36 \text{ MeV}$ ,  $\theta_\alpha = 90^\circ$  was taken to be  $2.25 \pm 0.26 \text{ mb}/\text{sr}$ , the average of four published measurements. Recently in this laboratory careful measurements have been made by Lerner and Marion<sup>35</sup> of the  $(p, \alpha)$  and  $(p, p)$  cross sections for both lithium and fluorine. The results are in agreement with earlier measurements, except for the  $\text{F}^{19}(p, \alpha_0)\text{O}^{16}$  cross section, which was found to be  $1.02 \pm 0.10 \text{ mb}/\text{sr}$  at  $E_p = 1.36 \text{ MeV}$ ,  $\theta_\alpha = 90^\circ$ . [By examining the published reports of measurements of the  $\text{F}^{19}(p, \alpha_0)\text{O}^{16}$  cross section, it is easy to see that the methods used could have produced erroneous results; a complete discussion is given in a separate report.<sup>35</sup>]

The best method of comparing the results of Paul *et al.* to those presented here is to consider the ratio of the cross sections for the reactions  $\text{F}^{19}(p, \alpha_0)\text{O}^{16}$  and  $\text{Li}^7(p, \alpha)\text{He}^4$ . This ratio has been carefully measured by three independent observers and their results are  $2.35 \pm 0.12$ ,<sup>34</sup>  $2.38 \pm 0.17$ ,<sup>35</sup> and  $2.60 \pm 0.15$ .<sup>36</sup> The weighted mean of these results yields

$$d\sigma[\text{F}^{19}(p, \alpha_0)\text{O}^{16}]/d\sigma[\text{Li}^7(p, \alpha)\text{He}^4] = 2.43 \pm 0.08$$

at  $\theta = 90^\circ$  and  $E_p = 1.36 \text{ MeV}$ . The value of the  $\text{Li}^7(p, \alpha)\text{He}^4$  differential cross section obtained in this work at  $\theta_\alpha = 90^\circ$  and  $E_p = 1.36 \text{ MeV}$  is  $0.56 \pm 0.05 \text{ mb}/\text{sr}$ . Using the cross-section ratio above to normalize the data of Paul *et al.* to the  $\text{Li}^7(p, \alpha)\text{He}^4$  cross section presented here yields for Paul's measurements  $\sigma(18.15-16.63) = 0.79 \pm 0.19 \mu\text{b}$ ,  $\sigma(18.15-16.90) = 0.39 \pm 0.12 \mu\text{b}$ , and  $\sigma(17.64-16.63) = 6.7 \pm 1.2 \mu\text{b}$  to be compared with the results presented in Eqs. (13), (16), and (17). These two sets of cross sections now agree within the quoted uncertainties. The weighted average of the four most recent measurements of the  $\text{Li}^7(p, \alpha)\text{He}^4$  cross section at  $\theta_\alpha = 90^\circ$  and  $E_p = 1.36 \text{ MeV}$  is<sup>35</sup>  $0.52 \pm 0.05 \mu\text{b}$ , a value close enough to that obtained in this work,  $0.56 \pm 0.05 \mu\text{b}$ , to obviate the necessity of renormalizing all the data presented here.

The highest-energy resonance that was observed in the  $\text{Li}^7(p, \gamma)\text{Be}^{8*} \rightarrow 2\alpha$  reaction occurs near an incident proton energy of 1.89 MeV corresponding to a Be<sup>8</sup> excitation energy near 18.9 MeV. This level has not been observed in the capture reaction,  $\text{Li}^7(p, \gamma)\text{Be}^8$  (ground state or 2.9 MeV). From an analysis of the cross section for the  $(p, p'\gamma)$  and  $(p, n)$  reactions, it has been concluded<sup>37</sup> that the level is formed by  $S$ -wave protons and has  $J^\pi = 2^-(T=0)$ . The level width has been estimated to be  $\Gamma > 500 \text{ keV}$ . This large level width value is derived in part from the anomaly ob-

<sup>35</sup> G. Lerner and J. B. Marion, Nucl. Instr. Methods **69**, 115 (1969).

<sup>36</sup> J. M. Freeman, R. C. Hanna, and J. H. Montague, Nucl. Phys. **5**, 148 (1962).

<sup>37</sup> H. W. Newson, R. M. Williamson, K. W. Jones, J. H. Gibbons, and H. Marshak, Phys. Rev. **108**, 1294 (1957).

served in the  $\text{Li}^7(p, p'\gamma)\text{Li}^7$  reaction in which the high-energy portion of the excitation curve is dramatically distorted as a result of the opening of the neutron channel at  $E_p=1.880$  MeV. Since a detailed analysis of the  $(p, p'\gamma)$  cross section, incorporating the Wigner cusp effect, has not yet been made, the large level width should not be regarded as certain. On the other hand, it seems difficult to reconcile the previous result for  $\Gamma$  with the present experiment, which indicates a much smaller value:  $\Gamma=150\pm 50$  keV. The shapes of the anomalies in the  $\text{Li}^7(p, \gamma)\text{Be}^{8*}\rightarrow 2\alpha$  cross sections, as shown in Figs. 5 and 6, are clearly inconsistent with a level width as large as 500 keV, even allowing for the possible effect of the opening neutron channel.

The cross section at an incident proton energy of 1.89 MeV will be taken as the weighted average of the two measurements:  $(d\sigma/d\Omega)_{\text{lab}}=0.238\pm 0.019$   $\mu\text{b}/\text{sr}$ . The direct-capture background can be estimated by the calculated value assuming only a Coulomb interaction in the initial state (i.e.,  $0.125\pm 0.01$   $\mu\text{b}/\text{sr}$ ) which yields a resonant cross section of  $(d\sigma/d\Omega)_{\text{lab}}=0.113\pm 0.022$   $\mu\text{b}/\text{sr}$ . If the level is formed by  $S$ -wave protons, the angular distribution of the breakup  $\alpha$  particles is isotropic. Including the laboratory-to-c.m. solid-angle correction gives

$$\sigma(18.9-16.63)=1.43\pm 0.28 \mu\text{b}. \quad (19)$$

The branching ratio is obtained from the data shown in Fig. 4(f). The measured differential cross sections are

$$(d\sigma/d\Omega)(18.9-16.63)=0.254\pm 0.021 \mu\text{b}/\text{sr},$$

$$(d\sigma/d\Omega)(18.9-16.90)=0.0832\pm 0.0087 \mu\text{b}/\text{sr}. \quad (20)$$

Subtracting the appropriate direct capture contribution yields

$$\frac{\sigma(18.9-16.63)}{\sigma(18.9-16.90)} = \frac{0.129\pm 17\%}{0.0762\pm 12\%} = 1.69\pm 20\%. \quad (21)$$

Therefore, the total cross section for the 18.9-16.90 transition is

$$\sigma(18.9-16.90)=0.85\pm 0.24 \mu\text{b}. \quad (22)$$

The appearance of a resonant  $\gamma$ -ray transition from the 18.9-MeV level to the 16-MeV levels of  $\text{Be}^8$  is consistent with the assignments  $J^\pi=1^-, 2^-, 3^-$  ( $T=0$ ). This level cannot decay to the first excited state of  $\text{Be}^8$  by an electric dipole transition since  $E1(\Delta T=0)$  transitions are forbidden in self-conjugate nuclei; however, the decay can take place by electric dipole emission to the  $T=1$  components of the 16-MeV levels of  $\text{Be}^8$ . Therefore, although it is not certain that this level is the same as the one observed in the  $(p, p'\gamma)$  and  $(p, n)$  reactions, it strongly indicates that the levels are identical.

### C. Calculation of $\gamma$ -Ray Transition Matrix Elements

The partial widths for the various  $\gamma$ -ray transitions can be calculated from the measured cross sections and the known widths of the levels. The c.m. width of the 17.64-MeV state in  $\text{Be}^8$  is<sup>11</sup>  $\Gamma=10.7\pm 0.4$  keV. The measured cross section for the 17.64-16.63 transition was  $8.62\pm 0.83$   $\mu\text{b}$ . Using the mean value of the branching ratio of  $(4.0\pm 0.9)\%$  yields partial widths of

$$\Gamma_\gamma=0.032\pm 0.003 \text{ eV} \quad (17.64\rightarrow 16.63),$$

$$\Gamma_\gamma=0.0013\pm 0.003 \text{ eV} \quad (17.64\rightarrow 16.90). \quad (23)$$

The multipole mixing ratio for the 17.64-16.63 transition is<sup>7</sup>  $\delta=-0.014\pm 0.013$ . Therefore, the reduced matrix elements for the 17.64-16.63 transition are, in Weisskopf units (W.u.),

$$\left. \begin{aligned} |M(M1)|^2 &= 1.48\pm 0.15 \text{ W.u.} \\ |M(E2)|^2 &= 7.8_{-7.4}^{+19.4} \text{ W.u.} \end{aligned} \right\} \quad (17.64\rightarrow 16.63). \quad (24)$$

The value of the matrix element for the 17.64-16.90 transition, assuming pure  $M1$ , is

$$|M(M1)|^2=0.15\pm 0.04 \text{ W.u.} \quad (17.64\rightarrow 16.90). \quad (25)$$

Partial widths and transition strengths can also be calculated for the  $\gamma$  transitions from the 18.15-MeV level of  $\text{Be}^8$ . The total width is<sup>11</sup>  $\Gamma=147$  keV. Using the measured cross sections  $\sigma(18.15-16.63)=0.65\pm 0.16$   $\mu\text{b}$  and  $\sigma(18.15-16.90)=0.52\pm 0.06$   $\mu\text{b}$  yields

$$\Gamma_\gamma=0.077\pm 0.019 \text{ eV}, \quad (18.15-16.63)$$

$$\Gamma_\gamma=0.062\pm 0.007 \text{ eV}, \quad (18.15-16.90) \quad (26)$$

and assuming pure  $M1$  transition gives

$$|M(M1)|^2=1.04\pm 0.26 \text{ W.u.}, \quad (18.15-16.63)$$

$$|M(M1)|^2=1.51\pm 0.17 \text{ W.u.} \quad (18.15-16.90). \quad (27)$$

Finally, the partial widths and transition strengths can be calculated for the level near 18.9-MeV excitation energy in  $\text{Be}^8$ . Here the calculations will only be approximate since neither the resonant energy nor the level width has been accurately determined. The level will be assumed to be  $J^\pi=2^-$  with an excitation energy of 18.9 MeV and a laboratory resonance width of 150 keV. Therefore,

$$\Gamma_\gamma=0.168 \text{ eV}, \quad (18.9-16.63)$$

$$\Gamma_\gamma=0.099 \text{ eV} \quad (18.9-16.90). \quad (28)$$

The transition matrix elements are

$$|M(E1)|^2=0.053 \text{ W.u.}, \quad (18.9-16.63)$$

$$|M(E1)|^2=0.045 \text{ W.u.} \quad (18.9-16.90). \quad (29)$$

It would be expected that the transition from the 18.9-MeV level to the 16.90-MeV level of Be<sup>8</sup> should be stronger than the transition from the 18.9-MeV level to the 16.63-MeV level since the 16.90-MeV level is believed to have a larger  $T=1$  component. However, considering the lack of precision in the cross-section measurements (e.g., the error in the branching ratio was  $\pm 20\%$ ) and the large uncertainties introduced in the subtraction of the direct-capture cross section at this energy, these results are in agreement with the assumption of nearly maximal isobaric spin mixing in the 16-MeV levels of Be<sup>8</sup>.

### V. CONCLUSION

The  $\gamma$ -ray transitions to the 16.63- and 16.90-MeV levels of Be<sup>8</sup> in the reaction  $\text{Li}^7(p, \gamma)\text{Be}^{8*}$  have been investigated over the range of incident proton energies 0.441–2.45 MeV. The 16.63-MeV level is populated at all proton energies in this range, and the nonresonant cross sections were compared successfully with the predictions of an extranuclear direct-capture process. The magnitude of the direct-capture cross section depends on the coefficients of fractional parentage (cfp's) linking the 16.63-MeV state to the ground state of Li<sup>7</sup>. Reasonable agreement between the calculated and experimental direct-capture cross sections was obtained using the cfp's calculated by Stephenson and Marion.<sup>29</sup> These cfp's were calculated from the intermediate-coupling shell-model wave functions of Barker<sup>12</sup>; therefore, they connect states having definite isobaric spin. The isobaric-spin wave function<sup>21</sup> for the 16.63-MeV level and the cfp's can be used to calculate the fractional parentage of the 16.63-MeV level. The cfp's connecting the 16.63-MeV level to the ground state of Li<sup>7</sup> are 0.239 for  $j=\frac{1}{2}$  and 0.643 for  $j=\frac{3}{2}$ . It should be noted that the results of Stephenson and Marion indicate that a large share of the fractional parentage of the 16.63-MeV state is contained in the excited states of Li<sup>7</sup>.

There have been several calculations of the expected  $\gamma$ -ray transition strengths to the 16-MeV levels of Be<sup>8</sup>. Paul<sup>10</sup> has calculated the single-particle transition strengths for  $p$ -shell protons and the following transitions:  $\frac{3}{2} \rightarrow \frac{3}{2}$ ,  $\frac{1}{2} \rightarrow \frac{3}{2}$ , and  $\frac{1}{2} \rightarrow \frac{1}{2}$ . The measured channel-spin mixing ratio at the 0.441-MeV resonance,  $r=3.2$ , indicates contributions from both  $p_{1/2}$  and  $p_{3/2}$  capture. It is probable that the 18.15-MeV level is also formed through both  $p_{1/2}$  and  $p_{3/2}$  capture. Since there are two possible values for the angular momentum of the proton in both the initial and final states, it is unlikely

that the transitions can be described successfully by unique single-particle transitions.

Barker<sup>12</sup> used the measured branching ratio (7%) for  $\gamma$ -ray transitions from the 17.64-MeV level to the 16.90- and 16.63-MeV levels to determine the isobaric spin mixing in the 1<sup>+</sup> levels. After determining the isobaric-spin mixing, Barker calculated other quantities [e.g.,  $\Gamma_\gamma(M1)$ , channel-spin mixing ratio, spectroscopic factors] for the 1<sup>+</sup> levels of Be<sup>8</sup>. The measurements of the strengths of the  $\gamma$ -ray transitions from the 18.15-MeV level to the 16-MeV levels of Be<sup>8</sup> reported here and by Paul<sup>10</sup> should provide the basis for a more accurate determination of the isobaric-spin mixing in the 1<sup>+</sup> levels of Be<sup>8</sup>.

Based on the meager knowledge of the properties of the 3<sup>+</sup> levels of Be<sup>8</sup>, the absence of any resonant  $\gamma$ -ray transitions from the 3<sup>+</sup> levels to the 2<sup>+</sup> levels of Be<sup>8</sup> cannot be explained. The possibility does exist that interference between the overlapping 3<sup>+</sup> levels causes the differential cross section at a laboratory angle of 120° to be small for the incident proton energies (2.10 and 2.30 MeV) at which the cross section was measured. It is also possible that the phase between the  $\Delta T=0$  and  $\Delta T=1$  components of the matrix elements are such that the 3<sup>+</sup>–2<sup>+</sup> transition probabilities are abnormally low. The measurement of the  $\gamma$ -ray transitions between the 3<sup>+</sup> and 1<sup>+</sup> levels, which have smaller isobaric-spin mixing than the 2<sup>+</sup> levels, could provide information on the nature of the 3<sup>+</sup> states in Be<sup>8</sup>.

Finally, the observation of  $\gamma$ -ray transitions from a state near 18.9 MeV to both 16-MeV levels of Be<sup>8</sup> with nearly equal strengths supports the model which attributes nearly equal  $T=0$  and  $T=1$  components in the wave functions of the 16-MeV states of Be<sup>8</sup>.

Therefore, all of the presently available evidence concerning the  $\gamma$ -ray transitions to the 16.63- and 16.90-MeV levels of Be<sup>8</sup> support the proposal that the 2<sup>+</sup> levels are very nearly single-particle in character and are highly mixed in isobaric spin and that the 1<sup>+</sup> levels exhibit some isobaric-spin mixing.

### ACKNOWLEDGMENTS

The authors would like to express their gratitude to Professor G. J. Stephenson, Jr. for his continued interest in this problem and for many helpful and stimulating discussions. They also wish to thank the University of Maryland Computer Science Center for making computer time available for calculations under the National Aeronautics and Space Administration Grant No. NsG-398.